Overshooting and undershooting subordination scenario for fractional two-power-law relaxation responses

Karina Weron,[1] Agnieszka Jurlewicz,[2] Marcin Magdziarz,[2,*] Aleksander Weron,[2] and Justyna Trzmiel[1]
[1]*Institute of Physics, Wrocław University of Technology, Wyb. Wyspiańskiego 27, 50-370 Wrocław, Poland*
[2]*Hugo Steinhaus Center, Institute of Mathematics and Computer Science, Wrocław University of Technology, Wyb. Wyspiańskiego 27, 50-370 Wrocław, Poland*

(Received 28 October 2009; revised manuscript received 5 March 2010; published 20 April 2010)

In this paper, we propose a transparent subordination approach to anomalous diffusion processes underlying the nonexponential relaxation. We investigate properties of a coupled continuous-time random walk that follows from modeling the occurrence of jumps with compound counting processes. As a result, two different diffusion processes corresponding to over- and undershooting operational times, respectively, have been found. We show that within the proposed framework, all empirical two-power-law relaxation patterns may be derived. This work is motivated by the so-called "less typical" relaxation behavior observed, e.g., for gallium-doped $Cd_{0.99}Mn_{0.01}Te$ mixed crystals.

DOI: 10.1103/PhysRevE.81.041123 PACS number(s): 05.40.Fb, 71.55.Gs, 77.22.Gm

I. INTRODUCTION

Wide-ranging experimental information, collected in both time and frequency domains, has led to the conclusion that the classical phenomenology of relaxation breaks down in complex materials such as supercooled liquids, amorphous semiconductors and insulators, polymers, disordered crystals, molecular solid solutions, glasses, etc. It has been found [1] that the relaxation behavior of such materials deviates considerably from the classical Debye pattern and is represented by low- and high-frequency fractional power-law dependences of the dielectric susceptibility $\chi(\omega)=\chi'(\omega)-i\chi''(\omega)$ on frequency

$$\chi(\omega) \sim (i\omega/\omega_p)^{n-1}, \quad \omega \gg \omega_p,$$

$$\Delta\chi(\omega) \sim (i\omega/\omega_p)^{m}, \quad \omega \ll \omega_p, \tag{1}$$

where $\Delta\chi(\omega)=\chi(0)-\chi(\omega)$, the exponents n and m fall in the range (0,1), and ω_p denotes the loss peak frequency.

A majority of the dielectric spectroscopy data can be characterized well enough by the empirical Havriliak-Negami (HN) function [2,3]

$$\chi_{\mathrm{HN}}(\omega) \propto \frac{1}{[1+(i\omega/\omega_p)^{\alpha}]^{\gamma}}, \quad 0<\alpha,\gamma\leq 1. \tag{2}$$

For $\alpha=1$ and $\gamma<1$, the above formula takes the form known as the Cole-Davidson (CD) function, for $\alpha<1$ and $\gamma=1$, it takes the form of the Cole-Cole (CC) function, and for $\alpha=1$ and $\gamma=1$, one obtains the Debye pattern. For $\alpha<1$, the HN function (2) possesses the power-law properties (1) with $n=1-\alpha\gamma$ and $m=\alpha$, and it fits the so-called typical relaxation behavior with the power-law exponents satisfying relation $m\geq 1-n$ [2,3]. For practical purposes, to fit the data exhibiting the less typical relaxation behavior with $m<1-n$, the HN function with parameters from the extended range, $0<\alpha<1$ and $0<\alpha\gamma<1$, has been proposed [2]. Unfortunately, only for $\gamma\leq 1$ the origins of the HN function (2) can be found within the fractional Fokker-Planck equation [4] and continuous-time random walk (CTRW) [5,6] approaches.

The experimental evidence shows that the set of relaxation data exhibiting the less typical two-power-law relaxation pattern with the low- and high-frequency power-law exponents satisfying relation $m<1-n$ cannot be neglected. Indeed, such a less typical behavior has been observed by us in gallium (Ga)-doped $Cd_{0.99}Mn_{0.01}Te$ mixed crystals (see Fig. 1 where sample frequency-domain data measured for the $Cd_{0.99}Mn_{0.01}Te:Ga$ at various temperatures are depicted). The sample of $Cd_{0.99}Mn_{0.01}Te:Ga$ used in this study was processed by the Bridgman method. The room-temperature net donor concentration, estimated from capacitance-voltage measurements performed with 1 MHz capacitance bridge, was found to be in the order of 10^{16} cm^{-3}. Gold Schottky contacts were thermally evaporated on the front side of the

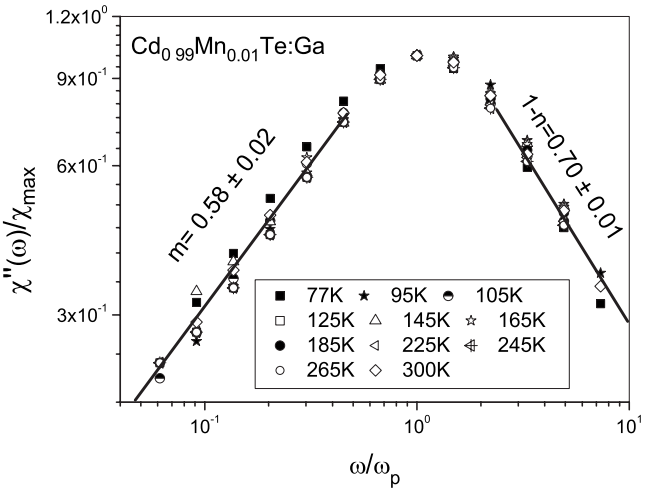

FIG. 1. Normalized imaginary susceptibility data obtained for gallium-doped $Cd_{0.99}Mn_{0.01}Te$ (log-log scale). Straight lines represent linear fits to data points. Values of the power-law exponents m and $1-n$ are equal to the slope coefficients estimated by the method of least squares.

*marcin.magdziarz@pwr.wroc.pl

sample. The measurements were performed using Novocontrol impedance analyzer. Dielectric response of the sample was measured in the frequency range from 0.2 Hz to 3 MHz at temperatures in the range of from 77 to 300 K. Presented results were obtained at zero bias after application of the ac probe signal amplitude equal to 10 mV.

The examined material belongs to semiconductors of group II-VI possessing deep metastable defects—the so-called DX centers (see [7] and references therein). Formation of such centers in $Cd_{1-x}Mn_xTe:Ga$ results from the bistability of Ga dopant which makes this mixed crystal an attractive material for holography and high-density data storage (optical memories). This fact motivates for increasing interest not only in experimental but also in theoretical studies [7,8] on relaxation behavior of semiconductor mixed crystals possessing the DX centers.

The aim of this paper is to derive a general class of the two-power-law relaxation responses covering and explaining the whole range of the observed pattern (1). A subordination approach, i.e., a transition from the physical time to a new operational time of the system, provides successful tools to study the anomalous diffusion processes [9–18]. Employing this subordination approach in Sec. II, we build a methodology to interpret both power-law exponents as well as the relationship between them in Sec. III. This is in contrast to earlier studies [19], where the fractional Fokker-Planck equation approach has led to the CC relaxation [formula (2) with $\gamma=1$] only. The technical parts of our derivation of over- and undershooting compound counting processes and corresponding subordinators are left for Appendixes A and B. Finally, we end with conclusions in Sec. IV, where discussion of our findings is presented.

II. SUBORDINATION APPROACH TO ANOMALOUS DIFFUSION

As far as the physical mechanism underlying the anomalous relaxation is concerned, the diffusion limit [5,6,10–12,15,20–22] of a CTRW should be considered. The CTRW process $R(t)$ determines the total distance reached by a random walker until time t. It is equal to the sum of independent and identically distributed random jumps R_i performed by the walker at random instants of time

$$R(t) = \sum_{i=1}^{\nu(t)} R_i, \tag{3}$$

where $\nu(t)$ denotes the random number of steps performed by the walker until time t. Diffusion front $\tilde{R}(t)$ of Eq. (3) is represented by the asymptotic behavior of the rescaled total distance $f(c)R(ct)$ when dimensionless time-scale coefficient c tends to ∞ and the space-rescaling function $f(c)$ is chosen appropriately

$$\tilde{R}(t) \overset{d}{=} \lim_{c\to\infty} f(c)R(ct). \tag{4}$$

(The symbol "$\overset{d}{=}$" means equal distributions.) Notice that $f(c)R(ct)$ is the total distance of the CTRW (3) corresponding to the rescaled spatiotemporal steps $[f(c)R_i, T_i/c]$, where $\{T_i\}$ denotes a sequence of interjump time periods that determine the counting process $\nu(t)$.

In the framework of linear-response theory [23,24], the temporal decay of a given mode k, representing excitation undergoing diffusion in the system under consideration, is given by the inverse Fourier transform of the diffusion front

$$\Phi(t) = \langle e^{ik\tilde{R}(t)} \rangle.$$

The relaxation function $\Phi(t)$ is related to the frequency-domain response by relation

$$\chi(\omega) \propto \int_0^\infty \exp(-i\omega t)\left(-\frac{d\Phi(t)}{dt}\right)dt,$$

and the high- and low-frequency power laws (1) correspond to the following short- and long-time behaviors of $\Phi(t)$:

$$1-\Phi(t) \sim (\omega_p t)^{1-n}, \quad \omega_p t \ll 1,$$

$$\Phi(t) \sim (\omega_p t)^{-m}, \quad \omega_p t \gg 1. \tag{5}$$

The resulting relaxation patterns are connected not only with stochastic properties of the jumps and the interjump times but also with a stochastic dependence between them. In the classical waiting-jump CTRW idea, in which the jump R_i occurs after the waiting-time period T_i, we have $\nu(t)=\nu_0(t)$, where

$$\nu_0(t) = \max\left\{ n: \sum_{i=1}^{n} T_i \le t \right\}$$

is the renewal counting process determined by the waiting times T_i's. However, the number of steps in Eq. (3) can be easily modified into

$$\nu(t) = \min\left\{ n: \sum_{i=1}^{n} T_i > t \right\} = \nu_0(t) + 1$$

if the jump-waiting CTRW scenario, in which a walker rests for time T_i after jumping on distance R_i, is taken into account. In case of the decoupled CTRW, i.e., when additionally the stochastic independence of the jump R_i and the waiting time T_i is assumed, this modification does not influence the resulting diffusion front and the corresponding type of relaxation [25]. But, if the coupled case [25] is considered, the waiting-jump and jump-waiting schemes may lead to essentially different relaxation patterns as we shall show in this paper.

In order to enlarge the class of diffusion scenarios in the CTRW approach to relaxation, the so-called clustered-jump random walks have been introduced and examined [5,6,25]. This type of coupled CTRWs follows from a stochastic generalization of the renormalization-group transformation idea applied to random walks [26,27]. Let us note that the renormalization-group theory, appearing frequently in physics and material science [28], reveals a plethora of phenomena that are scale invariant such as the polymer statistics of protein, the symbolic dynamics of DNA, the statistics of relaxation rates in complex (dielectric, magnetic, or mechanical) relaxing systems, etc.

The properties of the clustered-jump CTRW, which result originally from assembling the jumps from a randomly sized spatial cluster into a single renormalized jump, can be obtained equivalently [25] by replacing the classical renewal counting process in Eq. (3) with a specially constructed compound counting process. (For details, see Appendix A.) Namely, in the clustered-jump CTRW for the waiting-jump scheme, the number of jumps performed up to time t reads

$$\nu^U(t) = \nu_0(t) - U(t), \tag{6}$$

and since it is less than the number $\nu_0(t)$ in the classical case, it defines the undershooting compound counting process. For the jump-waiting scheme, the number of jumps performed up to time t exceeds $\nu_0(t)$ and is given by the overshooting compound counting process

$$\nu^O(t) = \nu_0(t) + O(t). \tag{7}$$

Formulas (6) and (7) reflect physical dependences (coupling) between the waiting time and the following jump and between the jump and the following resting time, respectively. It follows from the construction that the coupling terms $O(t)$ and $U(t)$ are related to the size of the last clustered spatiotemporal step performed before or at time instant t. Term $O(t)$ counts those elements of the clustered jump that would occur after time t and $U(t)$ those performed before or at t if the clustering procedure were not applied. The sum $U(t)+O(t)$ is hence equal to the (random) size of the considered cluster.

It strongly depends on distribution of the cluster sizes if the above counting processes influence (or not) the corresponding diffusion front. It appears [25] that clustering with finite-mean-value cluster sizes does not lead beyond the classical decoupled CTRW models. In particular, assuming additionally heavy-tailed distribution of the waiting times

$$\mathrm{Prob}(T_i \geq t) \sim (t/\tau_0)^{-\alpha} \ \text{as} \ t \to \infty \tag{8}$$

for some $0<\alpha<1$, $\tau_0>0$ and considering symmetric jumps R_i with finite-mean-square length $\langle R_i^2\rangle=\sigma^2>0$, independent of T_i, we obtain the diffusion front of the same subordinated form as in the classical decoupled case (see, e.g., [15])

$$\tilde{R}(t) \overset{d}{=} \sigma B(S_\alpha(t/\tau_0)), \tag{9}$$

where the parent process $B(s)$ is a Brownian motion and the operational time is given by

$$S_\alpha(t) = \inf\{s: L_\alpha(s) > t\}$$

for $L_\alpha(s)$ being a strictly increasing α-stable Lévy motion independent of $B(s)$. The parent process reflects the random properties of the jumps R_i. The operational time corresponds to the properties of the counting process and it strongly influences the kinetics of the system. Therefore, the relaxation properties of the system under the operational time are modified.

The probability distribution of the diffusion front (9) can be represented as well by a mixture of Gaussian and Lévy-stable laws. We have

$$\tilde{R}(t) \overset{d}{=} \sigma(t/\tau_0)^{\alpha/2}\mathcal{G}\Lambda_\alpha^{-\alpha/2}, \tag{10}$$

where $\mathcal{G}$ and Λ_α are independent random variables distributed according to the standard normal and completely asymmetric Lévy-stable laws, respectively. The corresponding relaxation pattern is given by the Mittag-Leffler (ML) relaxation function

$$\Phi_{\mathrm{ML}}(t) = E_\alpha(-(\omega_p t)^\alpha), \tag{11}$$

where $E_\alpha(x)$ is the Mittag-Leffler function [20,21,29] and $\omega_p=(\sigma|k|)^{2/\alpha}/\tau_0$ denotes a positive, characteristic material constant. In this case, the corresponding frequency-domain response $\chi(\omega)$ takes the CC form [20], which exhibits the power-law property (1) with $m=1-n=\alpha$.

The general class of the two-power-law relaxation responses follows from the scale-invariant clustering procedure characterized by a heavy-tailed cluster-size distribution with the tail exponent $0<\gamma<1$. In such a case, the operational time is modified by coupling between jumps and interjump times and becomes different than $S_\alpha(t)$. Moreover, the waiting-jump and jump-waiting schemes lead to two different limiting processes and, consequently, to different relaxation responses.

Indeed, for the jump-waiting scheme, we have shown [25] that

$$\tilde{R}^O(t) \overset{d}{=} \sigma(t/\tau_0)^{\alpha/2}\mathcal{G}\Lambda_\alpha^{-\alpha/2}\frac{1}{\mathcal{B}_\gamma^{1/2}}, \tag{12}$$

where $\mathcal{B}_\gamma$ is the generalized arcsine random variable, independent of $\mathcal{G}$ and Λ_α [defined as in Eq. (10)]. The above form of the diffusion front leads to the HN response [5], and it is equivalent to

$$\tilde{R}^O(t) \overset{d}{=} \sigma B(Z^O_{\alpha,\gamma}(t/\tau_0)), \tag{13}$$

where the operational time is given by $Z^O_{\alpha,\gamma}(t)=X^O_\gamma(S_\alpha(t))$. On the other hand, the waiting-jump scenario leads to [25]

$$\tilde{R}^U(t) \overset{d}{=} \sigma(t/\tau_0)^{\alpha/2}\mathcal{G}\Lambda_\alpha^{-\alpha/2}\mathcal{B}_\gamma^{1/2} \tag{14}$$

and as a consequence, to the generalized Mittag-Leffler (GML) response [6]. Equivalently,

$$\tilde{R}^U(t) \overset{d}{=} \sigma B(Z^U_{\alpha,\gamma}(t/\tau_0)) \tag{15}$$

with $Z^U_{\alpha,\gamma}(t)=X^U_\gamma[S_\alpha(t)]$. Here, $X^O_\gamma(s)=V_\gamma[Y_\gamma(s)]$ and $X^U_\gamma(s)=V^-_\gamma[Y_\gamma(s)]$ with $V_\gamma(y)$ being a strictly increasing γ-stable motion, $V^-_\gamma(y)=\lim_{x\to y-} V_\gamma(x)$ (the left-limit γ-stable process), and $Y_\gamma(s)=\inf\{y: V_\gamma(y)>s\}$. Moreover, $V_\gamma(s)$ and, consequently, $X^O_\gamma(s)$ and $X^U_\gamma(s)$, are independent of both $S_\alpha(t)$ and the parent process $B(s)$. To obtain diffusion fronts (9), (13), and (15), the scaling function has to be of the form $f(c)=[\Gamma(1-\alpha)c^{-\alpha}]^{1/2}$, where $\Gamma(\cdot)$ is the gamma function. For derivations of Eqs. (13) and (15), see Appendix B.

Formulas (13) and (15), presenting the anomalous diffusion processes in the subordinated version, are of a great importance for computer simulations of the walker's trajectories (Fig. 2) (for details see [16]). One can also use equiva-

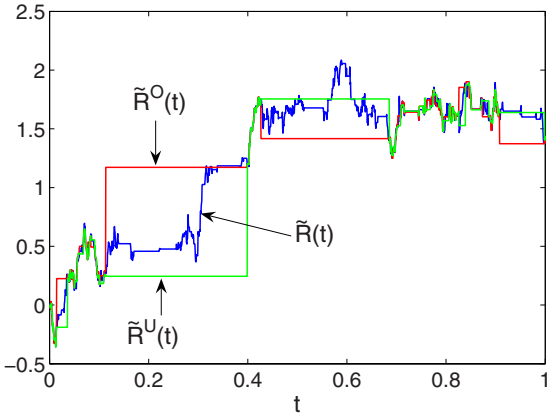

FIG. 2. (Color online) Sample paths of the diffusion fronts $\tilde{R}(t)$, $\tilde{R}^O(t)$, and $\tilde{R}^U(t)$ corresponding to the ML, HN, and GML relaxation responses, respectively. Parameters: $\alpha=0.9$, $\gamma=0.8$, $\sigma=\tau_0=1$.

lent forms of the compound subordinators $Z^O_{\alpha,\gamma}(t)$ and $Z^U_{\alpha,\gamma}(t)$,

$$Z^O_{\alpha,\gamma}(t) = S_\alpha(t) + O_\gamma[S_\alpha(t)], \tag{16}$$

$$Z^U_{\alpha,\gamma}(t) = S_\alpha(t) - U_\gamma[S_\alpha(t)], \tag{17}$$

where $O_\gamma(s)=X^O_\gamma(s)-s$ denotes the leap-over process [30,31] and $U_\gamma(s)=s-X^U_\gamma(s)$ the undershooting process. Formulas (16) and (17) reveal properties of the compound operational times $Z^O_{\alpha,\gamma}(t)$ and $Z^U_{\alpha,\gamma}(t)$ as over- and undershooting subordinators, respectively. The presence of coupling terms $O_\gamma(s)$ and $U_\gamma(s)$ reflects the random properties of the clustered complex system in which a given mode undergoes diffusion. Moreover, it indicates that the dissimilarity in the waiting-jump and jump-waiting schemes involves different modifications (stretching or contracting) of the operational time $S_\alpha(t)$ corresponding to the ML relaxation scenario (see Fig. 3).

III. TWO-POWER-LAW RELAXATION

The over- and undershooting subordination results in stretching and contracting of the operational time $S_\alpha(t)$ characteristic for the ML (or CC) relaxation mechanism

$$Z^U_{\alpha,\gamma}(t) \le S_\alpha(t) \le Z^O_{\alpha,\gamma}(t).$$

As a consequence, the ML scheme is extended within the subordination approach into two different relaxation scenarios covering the typical and less typical empirical relaxation patterns (see Table I). The overshooting subordinator (16) leads to

$$\Phi_{\rm HN}(t) = \int_0^\infty E_\alpha(-(\omega_p t)^\alpha x) h^O_\gamma(x)dx, \tag{18}$$

with $h^O_\gamma(x)=[\Gamma(\gamma)\Gamma(1-\gamma)]^{-1}x^{-1}(x-1)^{-\gamma}$ for $x>1$ and 0 otherwise. In this scenario, the corresponding frequency-domain response takes the form of the HN function (2) yielding the power-law property (1) with exponents $n=1-\alpha\gamma$ and $m=\alpha>1-n$, characteristic for the typical relaxation behavior (see Fig. 4).

In case of the undershooting subordinator (17), we obtain here a representation of the GML relaxation function [6]

$$\Phi_{\rm GML}(t) = \int_0^\infty E_\alpha(-(\omega_p t)^\alpha x) h^U_\gamma(x)dx, \tag{19}$$

with $h^U_\gamma(x)=[\Gamma(\gamma)\Gamma(1-\gamma)]^{-1}x^{\gamma-1}(1-x)^{-\gamma}$ for $0<x<1$ and 0 otherwise. [Notice that $h^O_\gamma(x)=x^{-2}h^U_\gamma(x^{-1})$.] In this scenario, the corresponding frequency-domain response cannot be expressed in an analytical form. Nevertheless, the power-law

TABLE I. Fractional relaxation scenarios, corresponding operational times (subordinators), and diffusion fronts.

Type of relaxation	Corresponding operational time	Corresponding diffusion front
Mittag-Leffler	$S_\alpha(t)$	$\tilde{R}(t) \overset{d}{=} \sigma B(S_\alpha(t/\tau_0))$
Havriliak-Negami	$Z^O_{\alpha,\gamma}(t)$	$\tilde{R}^O(t) \overset{d}{=} \sigma B(Z^O_{\alpha,\gamma}(t/\tau_0))$
Generalized Mittag-Leffler	$Z^U_{\alpha,\gamma}(t)$	$\tilde{R}^U(t) \overset{d}{=} \sigma B(Z^U_{\alpha,\gamma}(t/\tau_0))$

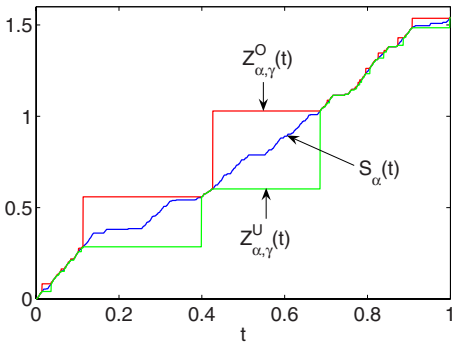

FIG. 3. (Color online) Sample paths of the operational times (subordinators) $S_\alpha(t)$, $Z^O_{\alpha,\gamma}(t)$, and $Z^U_{\alpha,\gamma}(t)$ corresponding to the ML, HN, and GML relaxation scenarios, respectively. We observe the following relationship $Z^U_{\alpha,\gamma}(t) \le S_\alpha(t) \le Z^O_{\alpha,\gamma}(t)$, which influences the speed of relaxation in the considered models. Parameters: $\alpha=0.9$, $\gamma=0.8$.

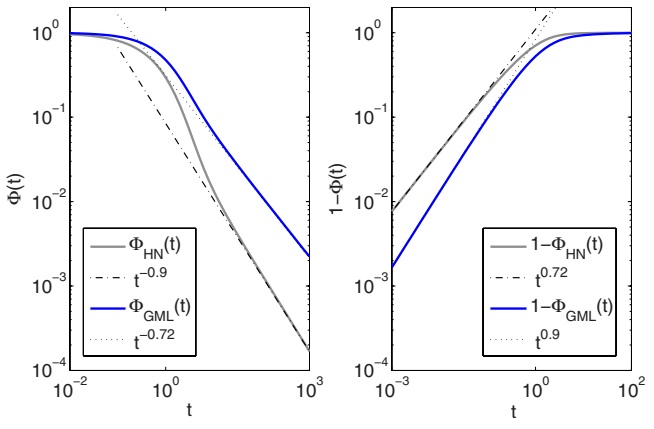

FIG. 4. (Color online) Sample time-domain representation of the HN and GML relaxation functions: (left panel) long-time and (right panel) short-time power-law behaviors. Parameters: $\alpha=0.9$, $\gamma=0.8$.

exponents and the relationship between them can be derived. We get the following: $n=1-\alpha$ and $m=\alpha\gamma<1-n$, which fit the less typical relaxation behavior (see Fig. 4).

The above relaxation functions can be represented also in the form of a weighted average of an exponential decay e^{-bt} with respect to the distribution of the effective-relaxation rate b. Namely, we have [6]

$$\Phi_{\mathrm{GML}}(t)=\int_0^\infty e^{-bt}g_{\mathrm{GML}}(b)db$$

for the following relaxation-rate probability density function

$$g_{\mathrm{GML}}(b)=\frac{\sin[\gamma\psi(b)](\pi b)^{-1}}{[(b/\omega_p)^{-2\alpha}+2(b/\omega_p)^{-\alpha}\cos(\pi\alpha)+1]^{\gamma/2}},$$

where

$$\psi(b)=\frac{\pi}{2}-\arctan\left(\frac{(b/\omega_p)^{\alpha}+\cos(\pi\alpha)}{\sin(\pi\alpha)}\right).$$

Similarly, we obtain [32,33]

$$\Phi_{\mathrm{HN}}(t)=\int_0^\infty e^{-bt}g_{\mathrm{HN}}(b)db$$

for

$$g_{\mathrm{HN}}(b)=\frac{1}{\pi b}\frac{\sin[\gamma\psi(b)]}{[(b/\omega_p)^{2\alpha}+2(b/\omega_p)^{\alpha}\cos(\pi\alpha)+1]^{\gamma/2}},$$

where here

$$\psi(b)=\frac{\pi}{2}-\arctan\left(\frac{(b/\omega_p)^{-\alpha}+\cos(\pi\alpha)}{\sin(\pi\alpha)}\right).$$

This result is in agreement with the idea of a superposition of the classical (exponential) Debye relaxations in the historically first attempt to nonexponential dielectric relaxation phenomena (see, e.g., [1]). The result follows from the fact that the ML relaxation function (11) can be expressed as a linear continuous superposition of decaying exponentials [34,35].

A complete understanding of the fractional two-power-law relaxation mechanism requires an explanation of the microscopic origins of the parameters α and γ. As far as α is concerned, the progress in understanding of this parameter has been already made few years ago (see [4] and the references therein). The parameter α arises naturally from the diffusion limit of a decoupled CTRW in which the interjump times obey distribution with the characteristic power tail (8) and the jumps are of a finite-mean-square length. This "fractal-time" random-walk picture [36], whereby a particle is trapped in a given configuration for an arbitrarily long time before executing a jump, immediately suggests that the parameter α is related to the anisotropy of the material on a microscopic scale. The microscopic anisotropy gives rise to a distribution of microscopic potential barrier heights which, in turn, give rise to a hierarchy of relaxation times not all of which have the same probability of occurrence. It can be, hence, concluded that the parameter α, characteristic for the ML relaxation, has its origin in random activation energy scenario [37].

Concerning interpretation of the parameter γ, some advances were made by Kalmykov *et al.* [4] in their generalization of the noninertial Fokker-Planck equation to the fractional kinetics. Replacing the partial derivative in the Fokker-Planck equation by a fractional operator of order γ, they succeeded in derivation of the HN function without any explanation of the relaxation mechanism hidden behind it. The authors [4] even doubted if the fractional-time random walk underlying the HN relaxation can be ever found. Contrary to that conclusion, we have succeeded in construction of such a CTRW scheme (and equivalent subordination scenario) that yields not only the HN response but also the GML pattern fitting the less typical relaxation behavior. Within the proposed approach, we have shown that the parameter γ arises from a scale-invariant structure of the complex systems and its origins are related to stretching and contracting of the operational time corresponding to the ML case.

IV. CONCLUSIONS

Using the subordination approach to anomalous diffusion, we have demonstrated how the well-known uncoupled CTRW, underlying the ML relaxation, can be generalized to a coupled CTRW yielding the two-power-law dielectric relaxation patterns with any exponent m and n falling in the range (0,1). We have hence shown that not only the ML ($m=1-n$) relaxation mechanism may be based on a fractional-time random walk. The result is of a particular interest in dielectric relaxation as it brings into light the fractional dynamics of both the typical ($m>1-n$) and less typical ($m<1-n$) responses. It shows that the two distinct classes follow from such a specific coupling between the jumps and the interjump times that stretches or contracts the operational time characteristic for the ML case. In other words, they follow from anomalous diffusion processes that lead to specific superpositions of the ML relaxation mechanisms.

Concluding, we have shown that betalike mixtures (18) and (19) of the Mittag-Leffler function provide two different relaxation functions that can explain the whole class of the two-power-law experimental results. Note that in agreement with the first statistical attempt to nonexponential relaxation phenomena, both relaxation functions may be equivalently expressed as a weighted average of an exponentially decaying function with respect to the effective-relaxation-rate distribution.

ACKNOWLEDGMENTS

The work of A.W. and J.T. was supported in part by the Contract No. POIG.01.03.01-02-002/08-00. M.M. acknowledges partial financial support by European Union within European Social Fund.

APPENDIX A: DERIVATIONS OF OVER- AND UNDERSHOOTING COMPOUND COUNTING PROCESSES

The construction of the clustered-jump CTRW is strictly connected with assembling the jumps and waiting times into clusters of random sizes $M_1, M_2, \ldots$. We assume that $\{M_j\}_{j\geq 1}$

is a sequence of independent and identically distributed positive integer-valued random variables and that this sequence is independent of the family of the spatiotemporal vectors $\{(R_i,T_i)\}_{i\geq 1}$. Then we transform the sequence of spatiotemporal steps $\{(R_i,T_i)\}_{i\geq 1}$ into a new family $\{(\overline{R}_j,\overline{T}_j)\}_{j\geq 1}$ by means of the following procedure:

$$(\overline{R}_j,\overline{T}_j)=\sum_{i=1}^{M_j}(R_{i+M_1+\cdots+M_{j-1}},T_{i+M_1+\cdots+M_{j-1}}). \tag{A1}$$

The clustered-jump CTRW process is defined as a coupled CTRW corresponding to $\{(\overline{R}_j,\overline{T}_j)\}_{j\geq 1}$. Coupling (the dependence between the jumps $\overline{R}_j$ and the waiting times $\overline{T}_j$) is determined by the distribution of cluster sizes M_j [25]. In details,

$$R(t)=\sum_{j=1}^{\overline{\nu}(t)}\overline{R}_j, \tag{A2}$$

where $\overline{\nu}(t)=\max\{n:\Sigma_{j=1}^{n}\overline{T}_j\leq t\}$ for the waiting-jump scheme, while $\overline{\nu}(t)=\min\{n:\Sigma_{j=1}^{n}T_j>t\}$ for the jump-waiting scenario. Equivalently, the clustered-jump CTRW process (A2) takes the form consistent with (3) in which the number of summands is given by the following compound counting process:

$$\nu(t)=\sum_{j=1}^{\nu_M[\nu_0(t)]}M_j. \tag{A3}$$

For the waiting-jump case $\nu_M(m)=\nu_M^U(m)=\max\{n:\Sigma_{j=1}^{n}M_j\leq m\}$ that leads to $\nu(t)$ in Eq. (A3) equal to the undershooting compound counting process $\nu^U(t)=\nu_0(t)-U(t)$ [Eq. (6)]. In the jump-waiting scheme $\nu_M(m)=\nu_M^O(m)=\min\{n:\Sigma_{j=1}^{n}M_j>m\}$ and, as a consequence, we obtain the overshooting compound counting process $\nu^O(t)=\nu_0(t)+O(t)$ [Eq. (7)]. Observe that $\nu^O(t)-\nu^U(t)=0(t)+U(t)=M_{\nu_M^O(m)}$, the size of that clustered jump for which the clustered interjump time period includes the time instant t.

APPENDIX B: DERIVATIONS OF OVER- AND UNDERSHOOTING SUBORDINATORS

In what follows, we prove that the mixture of standard normal and completely asymmetric Lévy-stable laws given in formula (10) has the same distribution as the diffusion front $\widetilde{R}(t)$ in Eq. (9). Using the fact that the Brownian motion $B(s)$ is 1/2-self-similar [and hence $B(s)\overset{d}{=}s^{1/2}B(1)$] and independent of the operational time $S_\alpha(t)$, we obtain

$$\sigma B(S_\alpha(t/\tau_0))\overset{d}{=}\sigma(S_\alpha(t/\tau_0))^{1/2}B(1), \tag{B1}$$

where $B(1)$ has the same distribution as $\mathcal{G}$ in Eq. (10). Moreover, by $1/\alpha$ self-similarity of the α-stable Lévy motion $L_\alpha(s)$, yielding $L_\alpha(s)\overset{d}{=}s^{1/\alpha}L_\alpha(1)$, we get for $s>0$,

$$\mathrm{Prob}[S_\alpha(t)\leq s]=\mathrm{Prob}[L_\alpha(s)\geq t]=\mathrm{Prob}\{[t/L_\alpha(1)]^\alpha\leq s\}. \tag{B2}$$

Therefore, $S_\alpha(t)$ is equal in distribution to $[t/L_\alpha(1)]^\alpha$, where $L_\alpha(1)$ has the same distribution as Λ_α in Eq. (10). Plugging this result into Eq. (B1), we obtain

$$\sigma B(S_\alpha(t/\tau_0))\overset{d}{=}\sigma(t/\tau_0)^{\alpha/2}(L_\alpha(1))^{-\alpha/2}B(1),$$

which gives the desired mixture of standard normal and completely asymmetric Lévy-stable laws.

Now, let us show that the overshooting diffusion front $\widetilde{R}^O(t)$ defined in Eq. (13) is equal in distribution to the mixture of laws (12). We have

$$\begin{aligned}\sigma B(Z^O_{\alpha,\gamma}(t/\tau_0))&\overset{d}{=}\sigma(Z^O_{\alpha,\gamma}(t/\tau_0))^{1/2}B(1)\\&\overset{d}{=}\sigma(X^O_\gamma(S_\alpha(t/\tau_0)))^{1/2}B(1).\end{aligned} \tag{B3}$$

Recall that $X^O_\gamma(s)=V_\gamma[Y_\gamma(s)]$, with $V_\gamma(y)$ being a strictly increasing γ-stable motion and $Y_\gamma(s)$ its inverse. Thus, the process $X^O_\gamma(s)$ is one-self-similar and hence $X^O_\gamma(s)\overset{d}{=}sX^O_\gamma(1)$. Therefore, using Eq. (B2), we obtain

$$\sigma\{X^O_\gamma[S_\alpha(t/\tau_0)]\}^{1/2}B(1)\overset{d}{=}\sigma(t/\tau_0)^{\alpha/2}[L_\alpha(1)]^{-\alpha/2}[X^O_\gamma(1)]^{1/2}B(1). \tag{B4}$$

Additionally, $X^O_\gamma(1)$ can be represented as $X^O_\gamma(1)\overset{d}{=}1+O_\gamma(1)$, where $O_\gamma(s)$ is the leap-over process. The random variable $O_\gamma(1)$ is Fisher-distributed with parameters $(1-\gamma,\gamma)$ [30]. Therefore, $O_\gamma(1)\overset{d}{=}G_1/G_2$, where G_1 and G_2 are independent Gamma-distributed random variables with respective parameters $1-\gamma$ and γ. Consequently,

$$X^O_\gamma(1)\overset{d}{=}1+O_\gamma(1)\overset{d}{=}\frac{G_1+G_2}{G_2}\overset{d}{=}\frac{1}{\mathcal{B}_\gamma},$$

where $\mathcal{B}_\gamma$ is distributed according to the beta distribution with parameters γ and $1-\gamma$, known also as the generalized arcsine distribution. Plugging the above result into Eqs. (B3) and (B4) leads us to the desired result.

To show that the undershooting diffusion front $\widetilde{R}^U(t)$ defined in Eq. (15) is equal in distribution to the mixture of laws (14), we use the fact that for every $0<s<t$,

$$\mathrm{Prob}[X^U_\gamma(t)\leq s]=\mathrm{Prob}[X^O_\gamma(s)\geq t]=\mathrm{Prob}[t/X^O_\gamma(1)\leq s].$$

Therefore,

$$X^U_\gamma(1)\overset{d}{=}\frac{1}{X^O_\gamma(1)}\overset{d}{=}\mathcal{B}_\gamma.$$

Then, the next steps of the proof are parallel to the case of the overshooting diffusion front $\widetilde{R}^O(t)$.

[1] A. K. Jonscher, *Dielectric Relaxation in Solids* (Chelsea Dielectrics Press, London, 1983).
[2] S. Havriliak, Jr. and S. J. Havriliak, J. Non-Cryst. Solids **172-174**, 297 (1994).
[3] A. K. Jonscher, *Universal Relaxation Law* (Chelsea Dielectrics Press, London, 1996).
[4] Y. P. Kalmykov, W. T. Coffey, D. S. F. Crothers, and S. V. Titov, Phys. Rev. E **70**, 041103 (2004).
[5] K. Weron, A. Jurlewicz, and M. Magdziarz, Acta Phys. Pol. B **36**, 1855 (2005).
[6] A. Jurlewicz, K. Weron, and M. Teuerle, Phys. Rev. E **78**, 011103 (2008).
[7] J. Trzmiel, K. Weron, and E. Placzek-Popko, J. Appl. Phys. **103**, 114902 (2008).
[8] J. Trzmiel, K. Weron, J. Janczura, and E. Placzek-Popko, J. Phys.: Condens. Matter **21**, 345801 (2009).
[9] I. M. Sokolov, Phys. Rev. E **63**, 011104 (2000); **66**, 041101 (2002).
[10] M. M. Meerschaert and H.-P. Scheffler, J. Appl. Probab. **41**, 623 (2004).
[11] M. M. Meerschaert, D. A. Benson, H.-P. Scheffler, and P. Becker-Kern, Phys. Rev. E **66**, 060102(R) (2002).
[12] M. M. Meerschaert and E. Scalas, Physica A **370**, 114 (2006).
[13] A. Piryatinska, A. I. Saichev, and W. A. Woyczynski, Physica A **349**, 375 (2005).
[14] I. M. Sokolov and J. Klafter, Phys. Rev. Lett. **97**, 140602 (2006).
[15] M. Magdziarz and K. Weron, Physica A **367**, 1 (2006).
[16] M. Magdziarz, A. Weron, and K. Weron, Phys. Rev. E **75**, 016708 (2007).
[17] A. Lubelski, I. M. Sokolov, and J. Klafter, Phys. Rev. Lett. **100**, 250602 (2008).
[18] M. Magdziarz, A. Weron, and J. Klafter, Phys. Rev. Lett. **101**, 210601 (2008).
[19] R. Metzler, E. Barkai, and J. Klafter, Phys. Rev. Lett. **82**, 3563 (1999).
[20] K. Weron and M. Kotulski, Physica A **232**, 180 (1996).
[21] R. Metzler and J. Klafter, Phys. Rep. **339**, 1 (2000).
[22] E. Gudowska-Nowak, K. Bochenek, A. Jurlewicz, and K. Weron, Phys. Rev. E **72**, 061101 (2005).
[23] R. Kubo, J. Phys. Soc. Jpn. **12**, 570 (1957).
[24] R. H. Cole, J. Chem. Phys. **42**, 637 (1965).
[25] A. Jurlewicz, Diss. Math. **431**, 1 (2005).
[26] M. O. Vlad, Phys. Rev. A **45**, 3600 (1992).
[27] M. O. Vlad and M. C. Mackey, Phys. Rev. E **51**, 3104 (1995).
[28] T. G. Dewey, *Fractals in Molecular Biophysics* (Oxford University Press, Oxford, 1997).
[29] V. M. Zolotarev, *One-Dimensional Stable Distributions* (American Mathematical Society, Providence, 1986).
[30] I. Eliazar and J. Klafter, Physica A **336**, 219 (2004).
[31] T. Koren, M. A. Lomholt, A. V. Chechkin, J. Klafter, and R. Metzler, Phys. Rev. Lett. **99**, 160602 (2007).
[32] J. V. Bertelsen and A. Lindgård, J. Polym. Sci., Polym. Phys. Ed. **12**, 1707 (1974).
[33] A. Jurlewicz, Appl. Math. (Warsaw, Poland) **30**, 325 (2003).
[34] R. Gorenflo and F. Mainardi, in *Fractals and Fractional Calculus in Continuum Mechanics*, edited by A. Carpinteri and F. Mainardi (Springer-Verlag, New York, 1997), pp. 223–276.
[35] D. Fulger, E. Scalas, and G. Germano, Phys. Rev. E **77**, 021122 (2008).
[36] W. Paul and J. Baschnagel, *Stochastic Processes from Physics to Finance* (Springer-Verlag, Berlin, 1999).
[37] B. J. West, M. Bologna, and P. Grigolini, *Physics of Fractal Operators* (Springer-Verlag, New York, 2003).